Sensors and Actuators B 212 (2015) 145–154

Contents lists available at ScienceDirect

Sensors and Actuators B: Chemical

journal homepage: www.elsevier.com/locate/snb

Zebra GC: A mini gas chromatography system for trace-level determination of hazardous air pollutants

Apoorva Garg[a], Muhammad Akbar[a], Eric Vejerano[b], Shree Narayanan[a], Leyla Nazhandali[c], Linsey C. Marr[b], Masoud Agah[a,*]

[a] VT MEMS Lab, Bradley Department of Electrical & Computer Engineering, Virginia Tech, Blacksburg, VA 24061, United States
[b] Department of Civil and Environmental Engineering, Virginia Tech, Blacksburg, VA 24061, United States
[c] SEPAC Lab, Bradley Department of Electrical & Computer Engineering, Virginia Tech, Blacksburg, VA 24061, United States

ARTICLE INFO

Article history:
Received 7 August 2014
Received in revised form
27 November 2014
Accepted 19 December 2014
Available online 2 February 2015

Keywords:
Micro gas chromatography
Environmental monitoring
Hazardous air pollutants

ABSTRACT

A ready-to-deploy implementation of a microfabricated gas chromatography (μGC) system characterized for detecting hazardous air pollutants (HAPs) at parts-per-billion (ppb) concentrations in complex mixtures has been described. A microfabricated preconcentrator (μPC), MEMS separation column with on-chip thermal conductivity detector (μSC-TCD), flow controller unit, and all necessary flow and thermal management as well as user interface circuitry are integrated to realize a fully functional μGC system. The work reports extensive characterization of μPC and μSC-TCD for target analytes: benzene, toluene, tetrachloroethylene, chlorobenzene, ethylbenzene, and p-xylene. A Limit of Detection (LOD) of ~1 ng was achieved, which corresponds to a sampling time of 10 min at a flow rate of 1 mL/min for an analyte present at ~25 ppbv. An innovative method using flow-manipulation generated sharp injection plugs from the μPC even in the presence of a flow-sensitive detector like a μTCD. The μGC system is compared against conventional automated thermal desorption–gas chromatography–flame ionization detector (ATD–GC–FID) system for real gasoline samples in simulated car refueling scenario. The μGC system detected five peaks, including three of the target analytes and required ~3 orders of magnitude lower sample volume as compared to the conventional system.

1. Introduction

Hazardous air pollutants, such as aromatic compounds and polycyclic aromatic hydrocarbons have serious environmental and health effects that are implicated in a variety of diseases in humans ranging from birth defects to cancer [1]. Toxic volatile organic compounds (VOCs) such as benzene and toluene found in gasoline, and xylene used in ink, rubber, and leather industries are of concern as they are present at elevated concentration due to their high vapor pressure. Exposure to these toxicants may cause adverse health effects. Most of these pollutants emerge from man-made sources and activities including emissions from automobile, refineries, factories, and power plants. To safeguard the health of exposed individuals and to ensure that the concentrations of these VOCs do not exceed the permissible exposure levels set through federal regulations, it is critical to monitor exposure to these compounds.

Among various analytical methods, gas chromatography (GC) has been the established method for assessing the presence and concentration of VOCs in the environment, and GC coupled to mass spectrometry (GC–MS) is one of the most accurate and widely used tool. In this technique, samples are first collected from the field through trap based systems such as sorbent tubes or canister and then are analyzed in a laboratory by trained technicians. This technique requires manual intervention and multiple steps including sampling, storage, and shipping before analysis, and therefore is susceptible to higher losses and has longer measurement cycles. Most of these drawbacks can be overcome by using portable, field-deployable, and real-time detection systems. There have been attempts at miniaturizing GC–MS systems [2,3], but such systems are still bulky, expensive, and consume high amount of power. Other real-time detection techniques involve using a sensitive photo-ionization detector (PID) [4] to realize a total VOC analyzer. PID-based systems suffer from selectivity issues and require filtering at the source which renders them ineffective and expensive for multi-compound analysis. Colorimetric tubes are another inexpensive and popular technique for VOC analysis which rely on a color change induced by the irreversible reaction between the sensing

* Corresponding author. Tel.: +1 540 231 2653.
E-mail address: agah@vt.edu (M. Agah).

http://dx.doi.org/10.1016/j.snb.2014.12.136
0925-4005/

Table 1
Summary and comparison of μGC systems.

Features	INTREPID system, University of Michigan, Ann Arbor [22]	μGC system, Arizona State University [20]	μGC system, CNR-IMM Institute for Microelectronics and Microsystems [19]	Zebra GC system, Virginia Tech
Sampling and injection	Hybrid 2-stage (sorbent tube + micro trap, Carbopack) Pros: Short sampling time and sharp injections Cons: Power consumption and trap cleaning time increases.	Sorbent tube packed with Carbopack Pros: High volume sampled Cons: High power consumption, long cleaning times and wide injection plug	Microfabricated cavity packed with adsorbent. Pros: Low power consumption Cons: Medium sample volume and wide injection plug	Microfabricated cavity with embedded pillars and TenaxTA coating Pros: Low power consumption, High surface area, very sharp injections Cons: Low sample volume
Separation	1-m, spiral channel (150 μm × 240 μm) PDMS coated micro-column, temperature controlled Separation Time: 1 min	Multiple configurations. 2-m & 19-m carbowax coated capillary columns Separation time: 3 min	0.5-m, spiral channel (800 μm deep) carbograph packed micro-column, temperature controlled Separation time: 10 min	2-m, rectangular channel (70 μm × 240 μm) PDMS coated micro-column, temperature controlled Separation time: 1 min
Detection	Chemi-resistor array. LODs – 0.48–2.2 ng. Pros: Identification of co-eluted compounds Cons: Sensor response varies with flow rate and temperature, and optimal operating point changes according to analyte	Tuning-fork. Sensitivity ~100 ppbv. Pros: Low power consumption and high selectivity Cons: Long response time	Metal-oxide semiconductor. Sensitivity ~5 ppbv Pros: High sensitivity Cons: Long-term drift, Long response time	μTCD embedded in separation column. LOD–1 ng Pros: High reliability, Integrated, Low cost Cons: Low selectivity
Integrated system	Carrier gas: Ambient-air Pros: High performance, selective, fast analysis Cons: High system power consumption expected due to conventional trap	Carrier gas: Ambient-air Pros: High selectivity Cons: Only one microfabricated component, high system power consumption expected	Carrier gas: Ambient-air Pros: All microfabricated components, Highly sensitive Cons: Detector drifts over time – calibration (weekly) and replacement (few months) required	Carrier gas: Helium Pros: All microfabricated components, monolithic integration, good performance, low cost, high reliability Cons: Low selectivity detector, low sample volumes

material and the analyte [5]. However, this technique requires human intervention, and its use is limited by slow response and large uncertainty. A more comprehensive solution for detection of VOCs is based on portable gas chromatography systems leveraging micro-fabricated components to achieve a small form factor, low power consumption, selectivity, and high sensitivity. Several commercial high performance portable gas chromatography systems [6,7] have been reported, but they are still bulky, energy inefficient, and expensive for real-time environmental monitoring applications. Such system limitations can be addressed to a reasonable extent by making them more application specific and using lower cost, batch-fabricated micro components.

Currently, considerable research efforts in the development of micro gas chromatography (μGC) systems are directed toward developing and optimizing high-performance microfabricated components such as preconcentrators (μPC) [8–10], separation columns (μSC) [11–13], and gas detectors [14–17]. However, integration of the various components is a critical yet underexplored aspect.

In this work, we present an innovative μGC architecture, which leverages monolithic integration of a separation column with micro-thermal conductivity detectors (μSC-TCD) [18] to minimize band broadening and chip-to-chip fluidic interfaces. The integration eliminates the need for a reference line and requires fewer external components. Another innovative aspect of this architecture is a method to perform very sharp injections from the μPC even in the presence of flow-sensitive gas detectors like TCD. This innovative system design relaxes constraints on the design of the μPCs by mitigating the effect of vapor desorption rate on the injection-plug width. The design enables us to achieve low detection limits suitable for environmental monitoring applications. We report in this current work the detailed system design, prototypal implementation, operation, and laboratory characterization of the proposed μGC system, dubbed Zebra GC. Table 1 provides a detailed comparison of four μGC systems, including Zebra GC, and highlights the features, advantages, and disadvantages of different system components. As seen, other reported μGC systems [19–23], while producing promising results, use individually fabricated chips which require extra effort to avoid compound condensation in cold spots. Also, some of these systems still use conventional components to achieve high performance which can lead to increased energy consumption or increased analysis time.

2. Zebra GC system architecture, fabrication and operation

The Zebra GC has two major units: (1) sampling and preconcentration, and (2) separation and detection. The μPC and μSC-TCD chips used in this work have integrated thin film heaters and sensors which are used for temperature control during desorption and separation. These microfabricated components are integrated with off-the-shelf flow controllers to implement GC flow cycles – loading, injection, analysis, and cleaning. An embedded platform, based on an 8-bit microcontroller (ATmega640, Atmel Corporation), is responsible for fluidic and thermal control. It also implements the user interface, signal processing, and data acquisition circuitry. The system is highly portable, battery powered, and easy to operate. It can be paired with a laptop for device control and data visualization through a Labview application.

2.1. Materials

Silicon wafers (4 in. dia., 500 μm thick, n-type, double side polished) and Borofloat wafers (4 in. dia., 700 μm thick, double side polished) were purchased from University wafers and Coresix Precision Glass (Williamsburg, VA), respectively. Tenax TA (80/100 mesh) and all other chemicals used for chromatographic testing were of analytical standard (>99% purity) and purchased from Sigma–Aldrich (St. Louis, MO). AZ 9260 photoresist and polydimethylsiloxane (PDMS or OV-1) were purchased from Micro-Chemicals (Germany) and Ohio Valley (Marietta, OH), respectively.

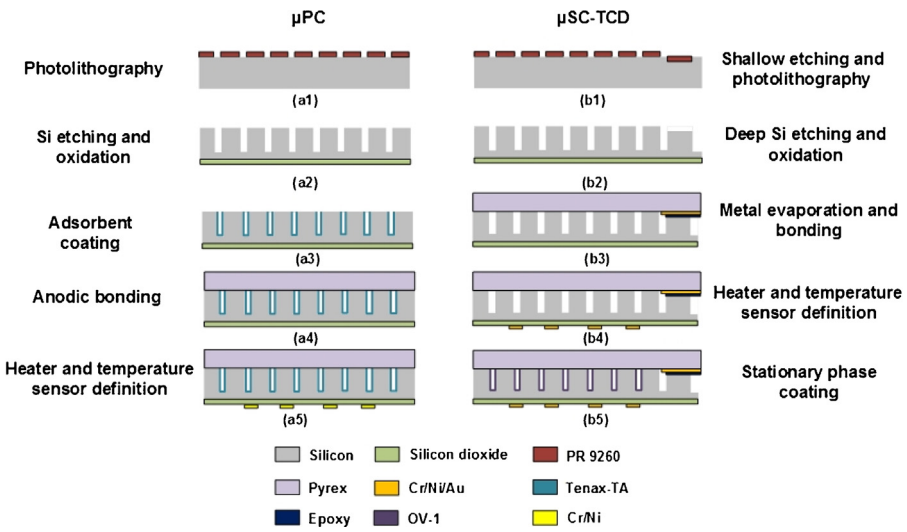

Fig. 1. Process flow for the fabrication of μPC and μSC-TCD with embedded temperature programming capability.

Fused capillary tubes (200 μm outer dia., 100 μm inner dia.) were purchased from Polymicro Technologies (Phoenix, AZ).

2.2. Microfabricated components

The fabrication process of the μPC and μSC-TCD has been depicted in Fig. 1 and described in our previous publications [18,24–28] in detail. The μPC is a 13 mm × 13 mm silicon-glass chip and consists of an array of high aspect ratio micro-posts inside its 1 cm square cavity. The micro-posts are realized by bulk micromachining of a 4 in. silicon wafer utilizing a deep reactive ion etching process to achieve a depth of 240 μm. A 1-μm thick plasma enhanced chemical vapor deposition (PECVD) oxide layer that acts as an insulator is deposited on the backside (Fig. 1 – a2). The wafer is then diced into individual chips. The micro-posts are then coated with a thin film (~200 nm) layer of Tenax TA adsorbent (Fig. 1 – a3) followed by capping with a Borofloat wafer via anodic bonding (Fig. 1 – a4). A 40 nm/230 nm of Cr/Ni stack is deposited which serves as a heater and temperature sensor on the backside of the chip using an e-beam evaporator (PVD-250, Kurt Lesker) (Fig. 1 – a5). The nominal resistance of the heater and sensor is around 15 Ω and 250 Ω, respectively. Finally, fused capillary tubes are inserted and epoxied to the inlet/outlet ports.

For the μSC-TCD, two-step anisotropic etching of silicon is performed. First, a shallow depth of 2–3 μm (Fig. 1 – b1) is achieved which prevents the contact between the metal interconnects on the Borofloat wafer and the walls of the separation column in silicon upon bonding. Second, a 2 m long, 70 μm wide and 240 μm deep channel is etched into silicon wafer (Fig. 1 – b2). TCD resistors are fabricated on a glass substrate using a lift-off process for a 40 nm/100 nm/25 nm Cr/Ni/Au stack deposited employing the e-beam evaporator. The glass and silicon substrates are then aligned and bonded together (Fig. 1 – b3). The heaters and temperature sensors are fabricated on the backside of the chip using stainless steel shadow mask (Fig. 1 – b4). Afterwards, the capillary tubes are epoxied into the inlet/outlet ports. The chip is finally coated with a thin layer (~250 nm) of OV-1 on the walls of the column channel (Fig. 1 – b5). An SEM image of the Tenax TA and OV-1 coating is

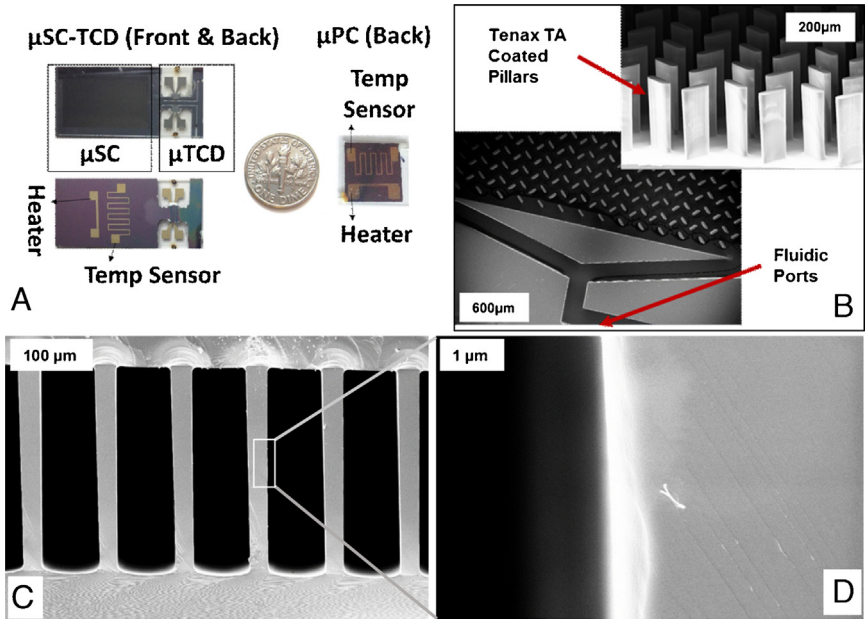

Fig. 2. (A) Micro-devices, (B) SEM images showing micro-posts in μPC, (C and D) polydimethylsiloxane coating on the interior wall of the column channel.

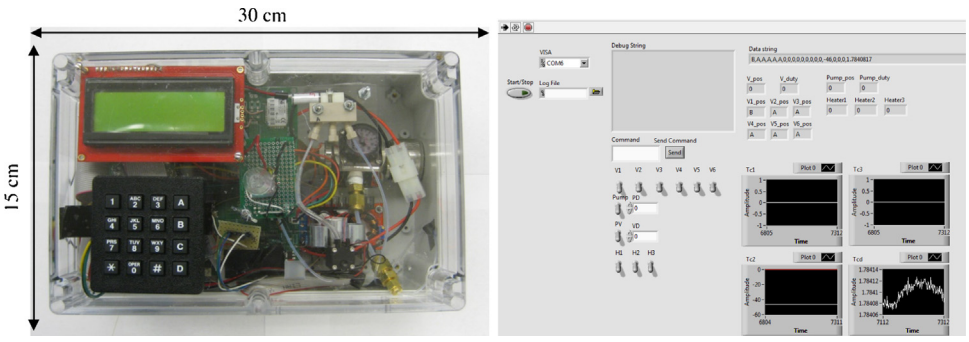

Fig. 3. (left) Zebra GC prototype implementation, (right) Labview application interface.

shown in Fig. 2. The optical image of all fabricated chips is shown in Fig. 2A.

2.3. Integrated electronic module

The microfabricated components, integrated with the pump (Parker Hannifin Co.), multi-way valves (The Lee Co.), and a portable helium cylinder, are controlled through an integrated electronic module managed by an 8-bit micro-controller, as shown in Fig. 4a. Latching valves are selected to optimize power consumption and controlled by applying a 100 ms 5 V DC pulse through an H-Bridge. The pump flow rate is adjusted by varying the pulse-width modulation (PWM) duty cycle, which is an important parameter during sample collection. The on-chip temperature sensors are connected in a 3-wire resistance temperature detector (RTD) configuration by using two well-matched current sources with a high precision 24-bit ADC. The reference voltage for the ADC is also generated using these matched current sources, through a precision resistor and applied to the differential reference pins of the ADC. This scheme ensures that the span of the analog input voltage remains ratiometric to the reference voltage and any error in the former due to temperature drift of the excitation current is compensated by the variation of the latter. On-chip heaters are controlled through PWM channels and a digital proportional control system is implemented as part of the embedded firmware, which generates different profiles for temperature reference signal based on the user input (initial temperature, step, ramp, final temperature).

The μTCD is connected in a Wheatstone bridge, driven by 7.5 V DC, with low noise thin film resistors (PF1260 series, Riedon Inc.). The differential signal is conditioned and filtered prior to feeding into an ultra-low noise 24 bit ADC (AD7793, Analog Devices). The signal is further filtered digitally, using an on-chip low pass modified Sinc3 filter that also provides 60 Hz rejection. The TCD, along with the entire system, is operated at a data rate of 10 Hz, which provides substantial resolution for the peaks.

2.4. System integration, interface, and operation

Microfabricated components along with the flow controllers, integrated electronic module, and user interface circuitry are assembled in a 30 cm (l) × 15 cm (w) × 10 cm (h) box, schematically shown in Fig. 4b. The box also houses a lithium ion battery (2200 mAh) pack and a small helium cylinder (95 mL, 2700 psi) to make the Zebra GC, shown in Fig. 3, highly portable (∼1.8 kg). The system can be operated in a manual or automatic mode using the LCD/Keypad based human–machine interface, which has a menu driven system. Once the mode is selected, the screen shows the state of the system in terms of valve positions, temperature readings, pump duty cycle, and sensor value. Sensor data can be visualized and recorded in the Labview application, which receives data packets through USB or Bluetooth interface.

Fig. 4c shows the timing diagram for the following automated stages: loading, injection, analysis, and cleaning. In loading stage, the pump applies negative pressure at the μPC outlet to load it with VOCs present in the air sample. Once sufficient sample is loaded in the μPC, the valves are switched to flow helium through the bypass path into the μSC-TCD. In order to ensure a sharp injection plug, the μPC is heated first at a rate of 25 °C/s to 200 °C without flow, and then the valve is switched to inject analytes into the μSC-TCD. The valve is switched back to the bypass path after injection and this stage typically lasts 10–12 s. Once the analytes are injected, they get separated and simultaneously identified in the μSC-TCD. This separation for the analytes of interest (BTEX) takes ∼1–2 min; the μSC can be operated at higher temperatures to reduce the analysis time or to resolve higher boiling compounds. Once the analysis phase is complete, the valves are switched back to flow helium at a rate of 3 mL/min through the μPC. The μPC is heated several times if necessary, to minimize residual analytes from the previous run. Typically, one temperature cycle (10–12 s) is sufficient to desorb the remaining analytes because of the high desorption efficiency of our silicon-based μPC.

3. Results and discussion

Individual components were tested and characterized before integrating them into the portable Zebra GC.

3.1. Integrated electronic module testing

The integrated electronic module primarily consists of temperature controllers, TCD interface, flow controllers, user interface, and data acquisition circuitry. Each module was tested and optimized separately before integration. For accurate temperature measurement, on-chip sensors were calibrated by placing the MEMS devices in a conventional GC (7890, Agilent, Palo Alto, CA) oven to characterize sensor resistance that responded linearly with respect to temperature with correlation coefficient of (R^2) >0.99. The calibration was completed by updating the firmware with calibration slope and offset, which were computed from the resistance vs. temperature data. The temperature profile required for the μPC is very different from that required for the μSC; the former requires heating at a high ramp rate (20–100 °C/s) to quickly desorb the analytes and generate a sharp injection plug, whereas the μSC requires heating at much lower ramp rates (0.2–1 °C/s) during the analysis phase to accelerate elution of high-molecular weight analytes. The μPC temperature reference was generated through the firmware, and a step input was given to heat the μPC to 200 °C, which was sufficient to completely desorb (∼ 99%) the analytes of interest. The heating ramp rate depends on the thermal mass, power dissipated, and heat losses. As shown in Fig. 5a, the maximum heating ramp rate of 25 °C/s was achieved for the μPC, by applying an 18 V DC across the heater resistance (15 Ω). Further increase in the voltage resulted in

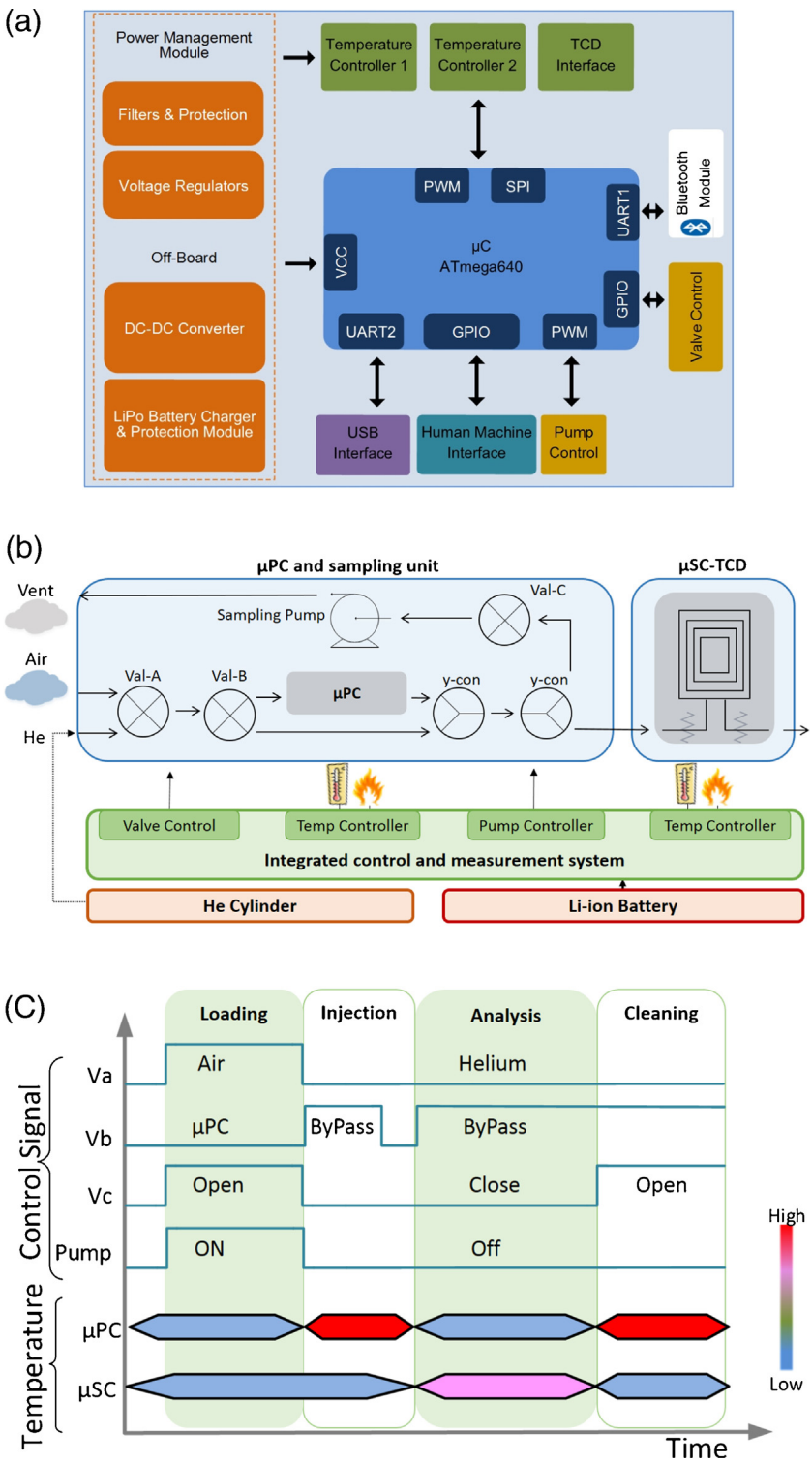

Fig. 4. (a) Integrated electronic module block diagram, (b) Zebra GC system block diagram, and (c) Operation cycles and timing diagram.

deterioration of the thin film heater due to high current density. As shown in Fig. 5b, the µSC was temperature programmed for ramp rates of 20 °C/min and 30 °C/min. The power consumptions were determined to be 0.5 W and 1.2 W for isothermal operation of the µSC at 45 °C and 65 °C, respectively.

The sensitivity of the µTCD detector was improved by increasing the signal-to-noise (S/N) ratio. The signal was amplified (Gain 32×), and the noise was reduced by filtering the signal and packaging the detector in a small aluminum box to mitigate the effects of ambient fluctuations. Once the measurement circuitry was tuned, noise measurements were made under normal operating conditions with the carrier gas flowing and the µTCD turned ON. The average peak-to-peak detector noise was 8.08 µV, measured using the technique reported in [29], for baseline signal captured for 10 s. The power consumption for the µTCD and pump operation was 280 mW and 165 mW, respectively. As shown in Table 2, the full measurement cycle of the Zebra GC consumes an average power of 2.75 W meaning that the battery can last up to 8 h (~110 full

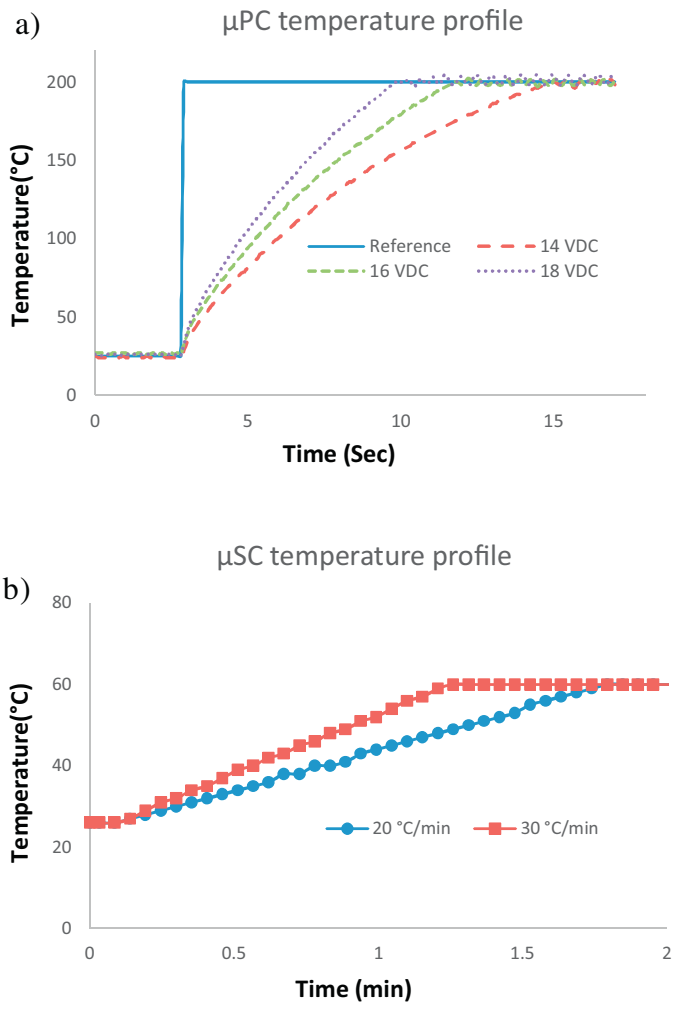

Fig. 5. (a) μPC temperature profile and effect of heater voltage on μPC heating. Average ramp rate – 25 °C/s, 20 °C/s and 15 °C/s; Average power consumption – 16 W, 13 W and 10.8 W; for heater voltage 18 V, 16 V and 14 V respectively. (b) μSC temperature profile for ramp rate 20 °C/min and 30 °C/min.

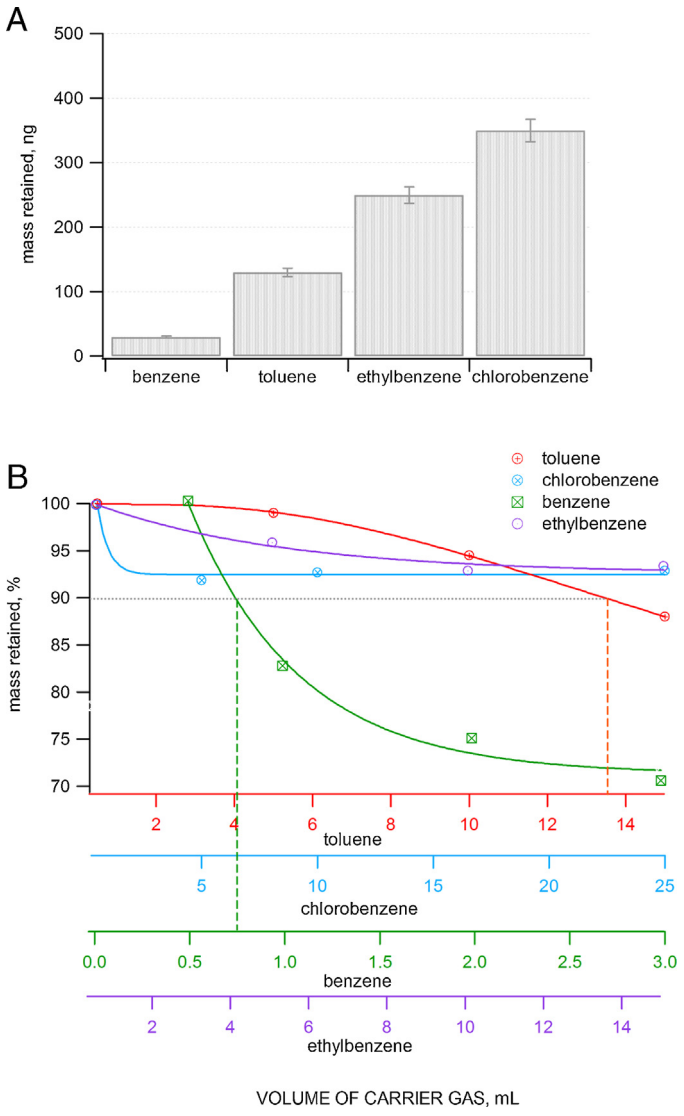

Fig. 6. (A) Maximum amount of test components retained in the μPC. (B) BV10 curves for benzene, toluene, chlorobenzene, and ethylbenzene. The *x*-axes are the volume of carrier gas needed to desorb the retained analyte. Dash lines represent breakthrough volumes, ethylbenzene and chlorobenzene have breakthrough volumes greater than the typical volume sampled (15 mL).

cycles). It is notable that in our current system, each helium refill (95 mL, 2700 psi) will last around 10,000 full cycles, meaning that the size of the helium cylinder and subsequently the Zebra GC can be considerably reduced.

3.2. *μPC testing*

For optimum operation, the μPC was characterized in terms of four important parameters: adsorption capacity, breakthrough volume, desorption peak width, and desorption efficiency. While evaluating the maximum adsorption capacity of the μPC, the effect of flow rate on the adsorption process was minimized by keeping it to a low value of 1 mL/min. Analytes were injected into the μPC from headspace in sealed 1 mL vials using a conventional GC autosampler module. The split ratio and the injection volume were changed to vary the amount of analyte introduced into the μPC. Analytes not retained by the adsorbent bed appeared as breakthrough peak which was allowed to return to the baseline prior to heating the μPC. The maximum adsorption capacity was defined as the mass retained in the μPC when the injection led to ~10% immediate breakthrough. Fig. 6A illustrates that the μPC can adsorb ~30–400 ng of analytes depending on their affinity to Tenax TA. The masses retained were ~30 ng, 130 ng, 240 ng, and 350 ng for benzene, toluene, chlorobenzene, and ethylbenzene, respectively. These results indicate that the μPC can retain a sufficient amount of compound well above the detection limit of our μTCD (~1 ng) and that it has higher affinity to high boilers as expected [26,30].

For breakthrough volume (*BV*) identification, about 4 ng of each analyte was loaded separately on the μPC at a flow rate of 1 mL/min and then 5, 10, 15, 25, and 30 mL of the carrier gas was passed through the μPC at the same flow rate. The μPC was subsequently heated and the volume of carrier gas which resulted in a 10% reduction in the total mass retained was noted. Fig. 6B illustrates that only benzene has a *BV* less than 1 mL; toluene has *BV* of 13 mL,

Table 2
System power consumption.

Operation stage	Average power (W)	Average time (min)	Major load
Loading	2.53	2	Pump, interface circuitry
Injection	16.5	0.2	μPC heating
Analysis	2.22	2	μTCD, interface circuitry
Cleaning	16.5	0.2	μPC heating
Full cycle	2.75	4.4	

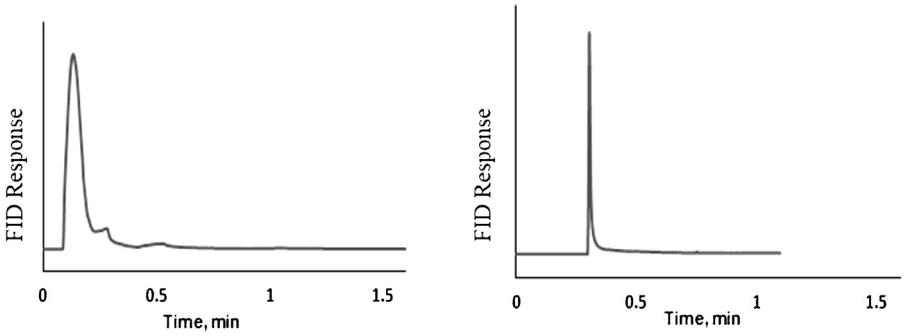

Fig. 7. (left) Desorption peak profile (PWHH ~4 s) generated from μPC by heating to 200 °C (ramp rate 25 °C/s) with flow rate 1 mL/min. (right) Desorption peak profile (PWHH ~350 ms) generated from μPC by heating to 200 °C (ramp rate 25 °C/s) with flow rate 2.5 mL/min, using flow manipulation technique.

while chlorobenzene and ethylbenzene have *BVs* above the typical volume sampled in our experiments (15 mL).

Another important parameter is the width of the desorption peak that can directly influence the chromatographic resolution achieved by the separation column. The initial desorption peak width attained on the μPC at a ramp rate of 25 °C/s and flow rate of 1 mL/min, was ~4 s. This was reduced by first heating the μPC without the carrier gas flowing and next, passing the carrier gas through when the chip temperature reaches 200 °C. As shown in Fig. 7, this flow-manipulation technique resulted in a reduction of the peak width at half height (PWHH) from 4 s to ~0.8 s. A minimum PWHH of ~350 ms was achieved when the desorption flow rate was increased to 2.5 mL/min. It is notable that 99% desorption efficiency for the analyte of interest was achieved by heating the μPC to 200 °C. The remaining amount was removed by subsequent heating of the μPC prior to another run to minimize carry over from the previous adsorption run.

3.3. μSC-TCD testing

The efficiency of the coated column was evaluated with the μTCD switched ON by applying a 7.5 V DC to the Wheatstone bridge. This voltage corresponds to a temperature of 80 °C for the μTCD and was measured with helium flowing, using the method reported previously [31]. The heated μTCD elevated the temperature of the column to 32 °C. The metric commonly used for the column performance is the height-equivalent-to-a-theoretical-plate (HETP),

$$\mathrm{HETP} = \frac{L}{N}$$

where L is the column length and N is the number of theoretical plates in the column. N is calculated experimentally from peak retention time (t_r) and peak width at half height ($w_{1/2}$).

$$N = 5.54\left[\frac{t_r}{w_{1/2}}\right]^2$$

The plate number was calculated over a range of column pressures using the method reported in our previous work [32]. The maximum plate number (optimum condition) observed was ~6200 for 2-m long column at 12 psi (flow rate of 0.7 mL/min).

Further, we tested the separation and identification of six VOCs using the column and its μTCD. The μSC along with the interface circuitry was installed inside the conventional GC and connected to the injection port and FID with fused-silica capillaries. A mixture of 6 compounds (headspace), containing benzene, toluene, tetrachloroethylene, chlorobenzene, ethylbenzene, and *p*-xylene, was injected by autosampler through the heated injection port (1 μL, 50:1 split ratio). The peaks were found to be well resolved and the separation required less than 2 min. Next, a calibration curve showing the output (peak area) of the μTCD as a function of the VOC injected mass was obtained. For that purpose, a headspace sample for each VOC was prepared and tested. The split ratio was varied from 120:1 to 50:1 based on the vapor pressure of the VOC. Injected volumes were varied from 0.5 μL to 4 μL, to achieve the mass injected in the range of 1–7 ng. Calibration curves showing the average peak area vs. injected mass for three injections are shown in Fig. 8. Results indicate a linear response of the μTCD for each VOC with a relative standard deviation (RSD) less than 10% for all cases. The R^2 was greater than 0.99 in all cases.

3.4. Integration of μPC and μSC-TCD

Once individual chips were tested and characterized, the μPC was connected upstream of the μSC-TCD to test the hybrid integration. The integration was expected to both improve and compromise the system performance of different aspects of the μGC. The compact design reduced the transfer lines, thereby reducing the formation of a cold spot that decreases efficiency. On the other hand, the optimal flow rate for operating the μPC and μSC was different; therefore, there was a trade-off in establishing the flow rate for the integrated system. The inlet port of the μPC was connected to the GC injector (280 °C, split ratio 50:1) and it was loaded with a mixture containing six compounds (headspace, 1 μL). For initial testing, the outlet port of μSC was connected to the FID detector of a conventional GC. The flow rate was set to 1 mL/min, for which the PWHH was measured to be 0.8 s from the μPC and the μSC exhibited well resolved peaks for the analytes of interest. As shown in Fig. 9, the six compounds were separated and identified in less than 2 min.

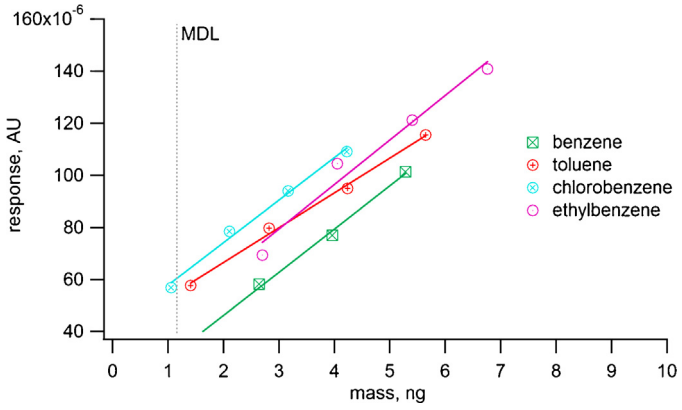

Fig. 8. Minimum detectable limit (MDL) for test compounds by μTCD.

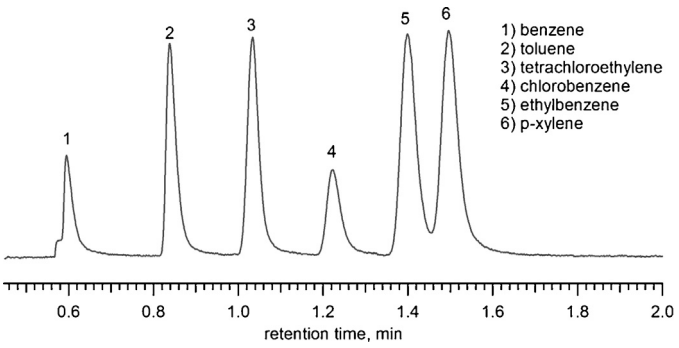

Fig. 9. FID response for separation of test compounds with integrated μPC and μSC. Injection performed using flow manipulation technique with μPC heated to 200 °C and desorption flow rate set to 1 mL/min.

TCD is sensitive to flow perturbation during the switching of carrier gas into the μPC; therefore, the integrated μTCD presented some challenges because of interference stemming from the injection of the analytes by the μPC. The problem was solved by adopting an innovative system architecture. As shown in Fig. 4a, an alternate flow path for the μPC was provided to maintain a steady flow in the μSC-TCD during the injection cycle. The fluidic resistance of the alternate flow path was matched closely with that of the μPC path to minimize flow perturbations while switching between the two paths. The new architecture decreased the μTCD stabilization time by one order of magnitude (from 1–2 min to 10 s) and ensured continuous flow of the carrier gas. As shown in Fig. 10b, 5 out of 6 compounds tested were easily identified.

3.5. Zebra GC testing, calibration and evaluation

The components of the Zebra GC were assembled as schematically shown in Fig. 4b. In addition to the integration of μPC and μSC-TCD mentioned above, a Y-connector was added between them to connect the small pump through a valve. The connector isolated the loading path of the μPC from the μSC-TCD, which reduced contamination in the μSC-TCD. This also permits loading at higher flow rates to the μPC since the high fluidic resistance in the μSC was avoided.

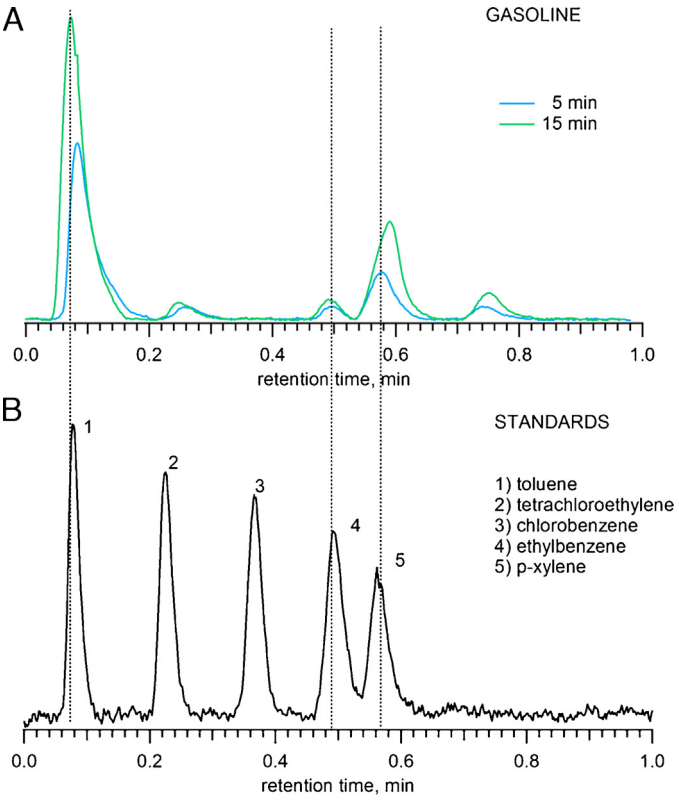

Fig. 10. Chromatogram of (A) gasoline vapor and (B) standards using Zebra GC.

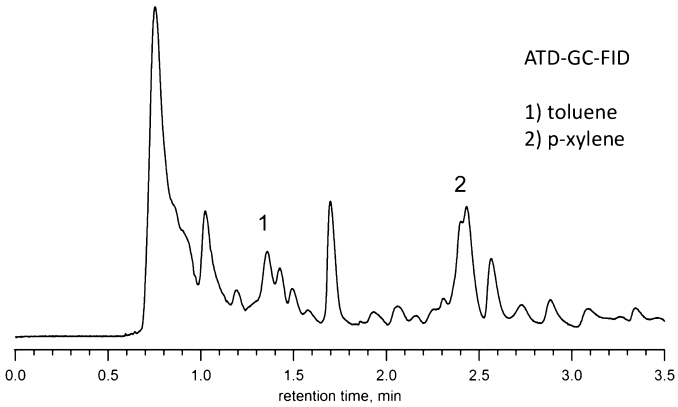

Fig. 11. Chromatogram of gasoline vapor sampled at ambient pressure and temperature using sorbent tubes containing ~200 mg of Tenax TA. Gasoline vapor was analyzed by thermal desorption coupled to GC–FID using conventional column containing (5% phenyl-, 95% dimethyl-polysiloxane). Desorption temperature and time were 300 °C and 25 min respectively. Toluene peak at ~1.4 min (16 ppmv) and p-xylene (14 ppmv) peak at ~2.4 min. Benzene and ethylbenzene not detected. Temperature programming: 35 °C, hold for 10 min, 5 °C/min to 150 °C, final hold time 1 min.

The Zebra GC was tested by loading the system with a mixture of five compounds (headspace), containing toluene, tetrachloroethylene, chlorobenzene, ethylbenzene, and *p*-xylene, injected by the GC autosampler through the heated injection port (1 μL, 40:1 split ratio) at 1 mL/min. As shown in Fig. 10b, calibration standards were generated with this method. The injected masses were ~2.7 ng, 3.2 ng, 1.8 ng, 1 ng, and 1.3 ng for toluene, tetrachloroethylene, chlorobenzene, ethylbenzene, and *p*-xylene respectively. These masses are equivalent to 10 mL loading of ~100 ppbv gas mixture, approximating a 10-min loading using a pump operated at 1 mL/min. The test was performed three times and retention times were highly repeatable with an RSD less that 1.3% for all analytes. The peak areas and peak heights had average RSDs less than 4.7% and 8%, respectively.

Finally, the fully assembled Zebra GC was evaluated in a simulated environment using gasoline as the source of exposure. The test atmosphere was generated by placing 50 mL of gasoline in a 100 mL beaker which was placed inside a large glass chamber (~4 L). Air was circulated inside the chamber but outside the gasoline beaker at 500 mL/min to simulate a car refueling scenario in which gasoline vapors displaced from the tank disperse in the atmosphere, where they may be inhaled [33]. The top of the chamber was kept open to the atmosphere and the chamber was allowed to be filled with vapors for 10 min. The vapors were sampled through the μGC, by keeping the system inlet close to the top of the chamber. Vapors were sampled under ambient temperature and pressure for two different sampling times, 5 and 15 min. To compare results with a conventional sampling system, gasoline vapors were also sampled using sorbent tubes packed with Tenax TA at a sampling flow rate of 69 mL/min for 3 h. Sorbent tubes were desorbed using a thermal desorption system coupled to a GC–FID (TD–GC–FID, Perkin-Elmer ATD 400). Toluene and *p*-xylene were identified at a concentration of 16 and 14 ppmv, respectively (Fig. 11). In both systems (Zebra GC and TD–GC–FID), benzene was not identified because it co-elutes with the other low-boiling point components in gasoline. Fig. 10a illustrates that the Zebra GC detected five peaks, three of which were identified as toluene, ethylbenzene, and *p*-xylene based on

retention times. Also, because Tenax TA has low affinity to benzene, the μGC system retained lesser mass of it compared to the other analytes. The sample volume collected and analyzed in the μGC was ~3 orders of magnitude lower than those collected on sorbent tubes. These results illustrate that the Zebra GC is capable of detecting and separating compounds with a much shorter sampling time and lower sample volume compared to conventional systems to complete one full cycle of analysis.

4. Conclusion

This study shows prototypal implementation of a μGC system suitable for environmental monitoring applications. The system leverages micro-machined components to achieve low power consumption (2.75 W) and fast analysis time (4.4 min). A Limit of Detection (LOD) of ~1 ng was achieved, which enables monitoring of HAPs at sub-100 ppbv concentrations. The fabricated prototype was functionally characterized and compared with a conventional ATD–GC–FID system for real gasoline samples. Future work will focus on: (i) comparing the accuracy and robustness of system through extended field tests in indoor and outdoor environments against conventional systems; (ii) design modification such as integrating a deep-etched μPC, enabling high sample volume, and utilizing semi-packed/multi-capillary columns for increased separation efficiency.

Acknowledgements

This research has been supported by the National Institute for Occupational Safety and Health under Award No. 1R21OH010330. We acknowledge the use of the facilities at the Institute for Critical Technologies and Applied Science, Nanoscale Characterization and Fabrication Laboratory (NCFL) at Virginia Tech in acquiring the FESEM images. Fabrication of the devices was performed at the Virginia Tech Microfabrication Cleanroom Facilities.

References

[1] S.T. Vater, S.F. Velazquez, V.J. Cogliano, A case study of cancer data set combinations for PCBs, Regul. Toxicol. Pharm. 22 (1995) 2–10.
[2] L. Li, T.-C. Chen, Y. Ren, P.I. Hendricks, R.G. Cooks, Z. Ouyang, Mini 12, Miniature mass spectrometer for clinical and other applications—introduction and characterization, Anal. Chem. 86 (2014) 2909–2916.
[3] L. Gao, Q. Song, G.E. Patterson, R.G. Cooks, Z. Ouyang, Handheld rectilinear ion trap mass spectrometer, Anal. Chem. 78 (2006) 5994–6002.
[4] A.N. Freedman, The photoionization detector: theory, performance and application as a low-level monitor of oil vapour, J. Chromatogr. A 190 (1980) 263–273.
[5] M. DuBois, K.A. Gilles, J.K. Hamilton, P.A. Rebers, F. Smith, Colorimetric method for determination of sugars and related substances, Anal. Chem. 28 (1956) 350–356.
[6] Agilent 490 Micro GC Product Information Page. Available at: http://www.chem.agilent.com/en-US/products-services/Instruments-Systems/Gas-Chromatography/490-Micro-GC/Pages/default.aspx (accessed July 2014).
[7] Inficon 3000 Micro GC Gas Analyzer Product Information Page. Available at: http://products.inficon.com/en-us/nav-products/Product/Detail/3000_Micro_GC_Gas_Analyzer?path=Products%2Fpg_ChemicalDetection (accessed July 2014).
[8] W.C. Tian, H.K.L. Chan, S.W. Pang, C.J. Lu, E.T. Zellers, High sensitivity three-stage microfabricated preconcentrator-focuser for micro gas chromatography, in: 12th International Conference on Transducers, Solid-State Sensors Actuators and Microsystems 2003, vol. 1, 2003, pp. 131–134.
[9] B. Alfeeli, M. Agah, MEMS-based selective preconcentration of trace level breath analytes, IEEE Sens. J. 9 (2009) 1068–1075.
[10] T. Wei-Cheng, S.W. Pang, L. Chia-Jung, E.T. Zellers, Microfabricated preconcentrator-focuser for a microscale gas chromatograph, J. Microelectromech. Syst. 12 (2003) 264–272.
[11] M. Agah, K.D. Wise, Low-mass PECVD oxynitride gas chromatographic columns, J. Microelectromech. Syst. 16 (2007) 853–860.
[12] S. Ali, M. Ashraf-Khorassani, L.T. Taylor, M. Agah, MEMS-based semi-packed gas chromatography columns, Sens. Actuators B: Chem. 141 (2009) 309–315.
[13] M.A. Zareian-Jahromi, M. Ashraf-Khorassani, L.T. Taylor, M. Agah, Design, modeling, and fabrication of MEMS-based multicapillary gas chromatographic columns, J. Microelectromech. Syst. 18 (2009) 28–37.
[14] R.E. Pecsar, R.B. DeLew, K.R. Iwao, Performance of a reduced volume thermal conductivity detector, Anal. Chem. 45 (1973) 2191–2198.
[15] S. Zimmermann, S. Wischhusen, J. Müller, Micro flame ionization detector and micro flame spectrometer, Sens. Actuators B: Chem. 63 (2000) 159–166.
[16] Detectors for capillary chromatography, Chem. Anal. 121 (1992).
[17] S.J. Martin, G.C. Frye, J.J. Spates, M.A. Butler, Gas sensing with acoustic devices, in: Ultrasonics Symposium, 1996 Proceedings, IEEE1996, vol. 1, 1996, pp. 423–434.
[18] S. Narayanan, B. Alfeeli, M. Agah, Two-port static coated micro gas chromatography column with an embedded thermal conductivity detector, IEEE Sens. J. 12 (2012) 1893–1900.
[19] S. Zampolli, I. Elmi, F. Mancarella, P. Betti, E. Dalcanale, G.C. Cardinali, et al., Real-time monitoring of sub-ppb concentrations of aromatic volatiles with a MEMS-enabled miniaturized gas-chromatograph, Sens. Actuators B: Chem. 141 (2009) 322–328.
[20] C. Cheng, F. Tsow, K.D. Campbell, R. Iglesias, E. Forzani, T. Nongjian, A wireless hybrid chemical sensor for detection of environmental volatile organic compounds, IEEE Sens. J. 13 (2013) 1748–1755.
[21] R.A. Iglesias, F. Tsow, R. Wang, E.S. Forzani, N. Tao, Hybrid separation and detection device for analysis of benzene, toluene, ethylbenzene, and xylenes in complex samples, Anal. Chem. 81 (2009) 8930–8935.
[22] W.R. Collin, G. Serrano, L.K. Wright, H. Chang, N. Nuñovero, E.T. Zellers, Microfabricated gas chromatograph for rapid, trace-level determinations of gas-phase explosive marker compounds, Anal. Chem. 86 (2013) 655–663.
[23] Y. Mohsen, H. Lahlou, J.-B. Sanchez, F. Berger, I. Bezverkhyy, G. Weber, et al., Development of a micro-analytical prototype for selective trace detection of orthonitrotoluene, Microchem. J. 114 (2014) 48–52.
[24] M. Akbar, M. Agah, A microfabricated propofol trap for breath-based anesthesia depth monitoring, J. Microelectromech. Syst. 22 (2013) 443–451.
[25] M. Akbar, D. Wang, R. Goodman, A. Hoover, G. Rice, J.R. Heflin, et al., Improved performance of micro-fabricated preconcentrators using silica nanoparticles as a surface template, J. Chromatogr. A 1322 (2013) 1–7.
[26] B. Alfeeli, V. Jain, R.K. Johnson, F.L. Beyer, J.R. Heflin, M. Agah, Characterization of poly(2,6-diphenyl-p-phenylene oxide) films as adsorbent for microfabricated preconcentrators, Microchem. J. 98 (2011) 240–245.
[27] H. Shakeel, M. Agah, Self-patterned gold-electroplated multicapillary gas separation columns with mpg stationary phases, J. Microelectromech. Syst. 22 (2013) 62–70.
[28] D. Wang, H. Shakeel, J. Lovette, G.W. Rice, J.R. Heflin, M. Agah, Highly stable surface functionalization of microgas chromatography columns using layer-by-layer self-assembly of silica nanoparticles, Anal. Chem. 85 (2013) 8135–8141.
[29] A Guide to Interpreting Detector Specifications for Gas Chromatographs. Available at: https://www.chem.agilent.com/Library/technicaloverviews/Public/5989-3423EN.pdf (accessed July 2014).
[30] B. Alfeeli, L.T. Taylor, M. Agah, Evaluation of Tenax TA thin films as adsorbent material for micro preconcentration applications, Microchem. J. 95 (2010) 259–267.
[31] S. Narayanan, M. Agah, Fabrication and characterization of a suspended TCD integrated with a gas separation column, J. Microelectromech. Syst. 22 (2013) 1166–1173.
[32] M. Akbar, S. Narayanan, M. Restaino, M. Agah, A purge and trap integrated microGC platform for chemical identification in aqueous samples, Analyst 139 (2014) 3384–3392.
[33] P.P. Egeghy, R. Tornero-Velez, S.M. Rappaport, Environmental and biological monitoring of benzene during self-service automobile refueling, Environ. Health Perspect. 108 (2000) 1195.

Biographies

Apoorva Garg received his B.Tech. degree in electrical engineering (power) from Indian Institute of Technology (IIT), Delhi, India, in 2009. He is currently working toward his M.S. degree in computer engineering at the Virginia Tech MEMS Laboratory, Bradley Department of Electrical and Computer Engineering, Blacksburg. His research interests include design and integration of micro gas chromatography systems.

Muhammad Akbar received the B.S. degree from the University of Engineering and Technology (UET), Peshawar, Pakistan, in 2006 and the M.S. degree from the University of Maryland, College Park, in 2010, both in electrical engineering. He is currently working toward the Ph.D. degree in the Virginia Tech MEMS Laboratory, Bradley Department of Electrical and Computer Engineering, Blacksburg. His research interests include the design, fabrication, and characterization of sensors for chemical and environmental applications using MEMS and nanotechnology.

Eric P. Vejerano received his B.S. degree in agricultural chemistry from the University of the Philippines Los Baños in 1999. He received his Ph.D. degree in chemistry from Louisiana State University in 2011. He is currently a post-doctoral researcher at the Department of Civil and Environmental Engineering at Virginia Tech.

Shree Narayanan holds a PhD in Electrical Engineering from Virginia Polytechnic Institute and State University (Virginia Tech), Blacksburg, VA, USA. His doctoral research at the VTEMS Laboratory, Virgina Tech, focused on the development of innovative gas detectors that can be monolithically integrated with gas chromatography separation columns without loss of sensitivity. He has a MS from the same department, for his thesis on the impedance measurement of biological cells. Prior

to joining Virginia Tech, he finished his Bachelors in Electronics and Communication Engineering from PES Institute of Technology, Bangalore, India.

Leyla Nazhandali received her B.S. degree in Electrical Engineering from Sharif University of Technology, Iran, in 2000 as an honor student. She, then, joined Advanced Computer Architecture Laboratory (ACAL) at the University of Michigan, Ann Arbor, where she pursued her graduate studies in Computer Engineering, receiving her M.S. and Ph.D. degrees in 2002 and 2006, respectively. She is currently an associate professor in the Bradley department of Electrical and Computer Engineering at Virginia Tech. Dr. Nazhandali is the recipient of the prestigious National Science Foundation CAREER award in 2008 and the winner of IEEE Real World Engineering Projects Contest. Her research interests are in low-power energy-constrained embedded system design, subthreshold-voltage architectures, secure embedded hardware design.

Linsey C. Marr received her B.S. degree in engineering science from Harvard College in Cambridge, Massachusetts in 1996. She received her Ph.D. degree in environmental engineering from the University of California at Berkeley in 2002. She trained as a post-doctoral researcher in Earth, Atmospheric, and Planetary Sciences at the Massachusetts Institute of Technology in Cambridge, Massachusetts. In 2003, she joined the faculty of Virginia Tech, where she is currently a professor of Civil and Environmental Engineering.

Masoud Agah received his B.S. and M.S. degrees in electrical engineering from Sharif University of Technology (SUT), Iran, in 1996 and 1998, respectively, and his Ph.D. degree from the University of Michigan, Ann Arbor, in 2005. He began his undergraduate studies in 1992 after being awarded by the President of Iran for achieving the first rank in the Nationwide Iranian University Entrance Examination. During his studies, he received numerous awards, including the Iranian Exemplary Graduate Student Honor, awarded by President Khatami in 1998. In 2000, he joined the NSF Center for Wireless Integrated MicroSystems (WIMS ERC), University of Michigan, where he developed MEMS-based gas chromatography columns for environmental monitoring applications. He joined the faculty of Virginia Tech in August 2005, where he is currently an associate professor in the Bradley Department of Electrical and Computer Engineering with a courtesy appointment in the Department of Mechanical Engineering. He is also a core faculty member of Virginia Tech-Wake Forest School of Biomedical Engineering and Sciences. He established the VT MEMS Laboratory in 2005 and has focused his research on environmental and biomedical applications of MEMS and nanotechnology. He is a senior member of the Institute of Electrical and Electronic Engineers (IEEE) and a member of the American Society for Mechanical Engineers (ASME).